Infrared optical properties of chromium nanoscale films with a phase transition

Robert Lovrinčić and Annemarie Pucci*
Kirchhoff-Institut für Physik, Universität Heidelberg, Im Neuenheimer Feld 227, 69120 Heidelberg, Germany
(Received 20 March 2009; revised manuscript received 12 June 2009; published 5 November 2009)

Thickness-dependent infrared spectra measured during growth of Cr on diamond C(100) under ultrahigh vacuum conditions reveal a structural phase transition from a discontinuous phase to the crystalline bulk one with Drude-type optical properties. The thickness of 2.5 nm of the observed phase transition well agrees with literature data on the theoretically predicted maximum size for stable fcc nanoclusters the formation of which should be supported on C(100) owing to a good lattice match. Below 2.5 nm, the spectral behavior surprisingly well corresponds to a Drude-Smith type dielectric function, which allows one to determine the conductivity for the discontinuous phase and to get quantitative information on the effect of coherent backscattering.

DOI: 10.1103/PhysRevB.80.205404 PACS number(s): 78.66.Bz, 68.55.−a, 73.61.−r, 81.15.Aa

I. INTRODUCTION

Cr is a bcc metal under normal conditions, but grown as thin films, it may show different phases.[1–3] For example, for Cr layers with $d=2.5$ nm on Au, an fcc structure was suggested from x-ray diffraction measurements.[1] Theoretically it was predicted, that for Cr nanoclusters with diameters $d<d_{\mathrm{crit}}=2.5$ nm the total energy for the fcc phase is lower then for the bcc phase due to the lower surface energy.[4] In Ref. 5 the fcc structure of Cr nanoclusters below the critical size of ~2.5 nm was proven by x-ray diffraction from cluster aggregates and by transmission electron microscopy.

Because of its good adhesion, Cr is frequently used as interlayer for metallization. For example, the system Cr on diamond is of special interest for new kinds of detectors in high-energy physics.[6] Despite the manifold application of ultrathin chromium layers, there is only little knowledge on the relationship between Cr thickness and conductivity. To obtain such information we performed systematic growth experiments in ultrahigh vacuum (UHV) with low-deposition rates and *in situ* monitoring of infrared (IR) spectra with high-photometric sensitivity. We used diamond substrates since they are relevant for the development of new detectors in high-energy physics. Moreover, diamonds are insulators and transparent in the IR, which allows optical conductivity measurements. In general, IR spectroscopy of metal nanofilms and nanoparticles measures the excitation spectrum of free-charge carriers. This spectrum is determined by the electrical conductivity of the metal and by the morphology of the nanoparticle system.[7–9] IR spectroscopy is a sensitive tool for conductivity measurements with the big advantage that electrical contacts are not necessary. Furthermore, related to their different influence on the IR spectral shape, it is possible to separate changes of different conductivity parameters (i.e., plasma frequency and relaxation rate).[10,11]

IR spectra measured during metal-film growth are quite different for different growth regimes (e.g., island-like growth[7] and layer-by-layer growth[12]). IR transmittance spectra for smooth layers can be perfectly described with the Drude model for the dielectric function. On the other hand, for metal-island films, the typical IR tail of the surface plasmon polariton excitation is observed.[7] During further metal deposition, with increasing lateral island size and decreasing island distances, this excitation shifts to lower frequencies until the percolation threshold is reached where a nearly frequency independent IR transmittance appears.[13] Concerning the IR spectral development, the growth of Cr on C(100) qualitatively resembles to the system Pb on Si(111)7×7, where a discontinuous phase is formed in the beginning and a transition to the ordered crystalline phase takes place at a certain thickness.[14] For Pb on Si(111)7×7 that transition thickness corresponds to an energetically favored island height and is related to quantum size effects.[12,14–16] Recent elaborated x-ray studies revealed the nature of the discontinuous phase as a dense packing of nanocrystals.[17] This phase shows a nearly linear, frequency independent decrease in IR transmittance with average film thickness, which could not be further analyzed because of a rather low signal-to-noise ratio.[12] In this chromium-film study, thanks to an improved signal-to-noise ratio, detailed analysis of IR spectra of the discontinuous phase is possible and the thickness-dependent conductivity can be derived.

II. IR PROPERTIES OF CR AND CONDUCTIVITY MODELS

The IR properties of bcc Cr can be reasonably described by the Drude model for the (relative) dielectric function,

$$\epsilon(\omega) = \epsilon_\infty - \frac{\omega_p^2}{\omega^2 + i\omega\omega_\tau}, \tag{1}$$

with the background permittivity ϵ_∞, usually set to unity in the IR, and the two Drude parameters plasma frequency $\omega_p = \sqrt{ne^2/(\epsilon_0 m_{\mathrm{eff}})}$ and relaxation rate $\omega_\tau = 1/\tau$ (ϵ_0 is the permittivity of vacuum). The corresponding complex optical conductivity $\sigma(\omega)$ is related to $\epsilon(\omega)$ by

$$\sigma(\omega) = -i[\epsilon(\omega) - \epsilon_\infty]\epsilon_0\omega. \tag{2}$$

As it follows from optical data for bulk Cr in Ref. 18, interband contributions can be neglected up to $\omega_{\max} \approx 1500\ \mathrm{cm}^{-1}$, i.e., up to this wave number the reported data well correspond to the Drude model with the parameters 36 650 cm^{-1} and 440 cm^{-1} for ω_p^{bulk} and $\omega_\tau^{\mathrm{bulk}}$, respectively.

Continuous ultrathin metal films in the mid IR can be well described with the Drude model, if ω_p and ω_τ are considered

as thickness-dependent parameters.[8,10,12,19] A thickness dependence of ω_τ is related to the scattering of conduction electrons at surfaces [classical size effect (CSE)].[20] The CSE leads to a roughness-dependent surface contribution $\omega_\tau^s(d)$ that is proportional to the inverse film thickness $1/d$. Additionally, crystalline defects in the film may differ from sample to sample. Scattering at defects might be more pronounced in as grown ultrathin films and, according to Matthiessen's rule,[21] might furthermore increase the relaxation rate by ω_τ^d. Hence, the thickness-dependent total relaxation rate is

$$\omega_\tau(d) = \omega_\tau^{\text{bulk}} + \omega_\tau^s(d) + \omega_\tau^d(d). \tag{3}$$

The change in ω_p with thickness in thin films arises from quantum size effects,[22] contributions from surface states,[23] and depolarization effects.[24] The Drude model (in the refined version by Sommefeld) is based on the relaxation time approximation. The collisions are assumed as infinitely short, as independent from each other, and as completely effective in obliterating any information about the electron configuration before the collisions. The last assumption means the complete loss of phase coherence and the destruction of the electron wave packet and, thus, more or less overestimates the efficiency of collisions.[25] To describe different cases, generalizations of the Drude model were adopted, e.g., the extended classical approach as suggested by Smith[26] that has recently been applied with great success for the description of thin particle films near the percolation threshold in the IR[27] and terahertz regime.[28–30] The Drude-Smith model basically assumes that phase coherence is completely lost after a series of collisions. Supposing persistence of velocity after the first collision (single-scattering approximation[26]) the complex dielectric function of the Drude-Smith model reduces to

$$\epsilon(\omega) = \epsilon_\infty - \frac{\omega_p^2}{\omega^2 + i\omega\omega_\tau}\left[1 + c\frac{\omega_\tau}{(\omega_\tau - i\omega)}\right]. \tag{4}$$

Here, in classical terms, the coefficient c represents that fraction of the electron's velocity in forward direction that, on average, is retained after a collision. This is the so-called memory or persistence of velocity effect. For elastic collisions, the parameter c corresponds to the expectation value of $\cos(\theta)$ where θ is the scattering angle. Accordingly, $c=0$ means isotropic scattering which gives a Drude-type metal and $c=-1$ means full backscattering of electrons, which corresponds to an insulator. Extrapolation to the static limit gives the dc conductivity

$$\sigma_{dc} = (1+c)\epsilon_0\omega_p^2/\omega_\tau. \tag{5}$$

III. EXPERIMENTAL

The experiments were performed in an UHV chamber with a base pressure of $1\cdot10^{-10}$ mbar and $2\cdot10^{-10}$ mbar during Cr deposition. The substrate was a commercial CVD diamond C(100) single crystal, supplied by *Element 6*, with dimensions $5\times5\times0.5$ mm^3. Prior to transfer into UHV it was cleaned in a boiling 1:1:1 solution of $HNO_3:H_2SO_4:HClO_4$. This treatment was carried out to remove amorphous carbon,[31] additionally leading to an oxygen terminated $p(1\times1)$ surface. Once transferred into UHV, the diamond was heated to 350 °C for several hours. Afterward, a LEED pattern was observed indicating a well prepared C(1 0 0)1×1 surface. Cr was deposited by an electron-beam evaporator (*Omicron*) at a rate of about 1 Å/min from a tungsten crucible. The rate was calibrated with a quartz-micro-balance before and after the experiment, which leaves an error of 10% in thickness and, consequently, of at least 5% in the fit parameter plasma frequency. The average film thickness was calculated from the measured average deposition rate and the time using the bulk density of Cr(7.14 g/cm^3).

During deposition the substrate was kept at room temperature. The IR spectrometer (*Bruker IFS 66 v/S*) and the HgCdTe (MCT) IR detector were coupled to the UHV chamber via KBr windows, so the spectra were taken during film growth. The spectral resolution was 8 cm^{-1}, data acquisition for one spectrum took about 45 s (corresponding to a thickness change of less than 1 Å during one spectrum). All spectra are relative transmittance measurements at normal incidence (electric field parallel to the layer) with the bare diamond as reference.

Ex situ atomic force microscopy (AFM) measurements were performed immediately after exposure to air with a Multimode scanning probe microscope (*Veeco SPM*) in contact mode.

IV. RESULTS AND DISCUSSION

Figure 1(a) shows the development of the relative transmittance during Cr deposition for various selected frequencies. According to the spectral development with thickness, three different phases (I, II, III) can be distinguished [see Fig. 1(a)]: In phase I, up to ~0.5 nm, no change in transmittance is observed. Such behavior is typical for the formation of a non-conductive wetting layer.[12] In phase II, up to ~2.5 nm, the transmittance is almost frequency independent, but decreases linearly with increasing d. For such ultrathin films (optical thickness $\ll$ wavelength), Fresnel's equations give a transmittance change that is linearly proportional to thickness and to the real part of the dynamic conductivity.[9] Thus, from that linear change it follows that the IR dynamic conductivity of phase II seems not to change with thickness, which is clearly different to metal films with qualitative changes in their morphology during growth. Moreover, the frequency-independent spectrum of phase II is typical for metal-particle systems at percolation. In metal-island films before percolation, the formation of separated metal islands usually is indicated by a transmittance with negative slope vs frequency, which is explained as the red tail of particle plasmon resonances.[7,32] The interaction between particles produces a red shift of the low-frequency tail of the optical absorption.[33]

For film growth via metal-island formation, percolation occurs at a certain average thickness and is not extended to a thickness range of several monolayers. The denser the nucleation centers for island formation the lower the average

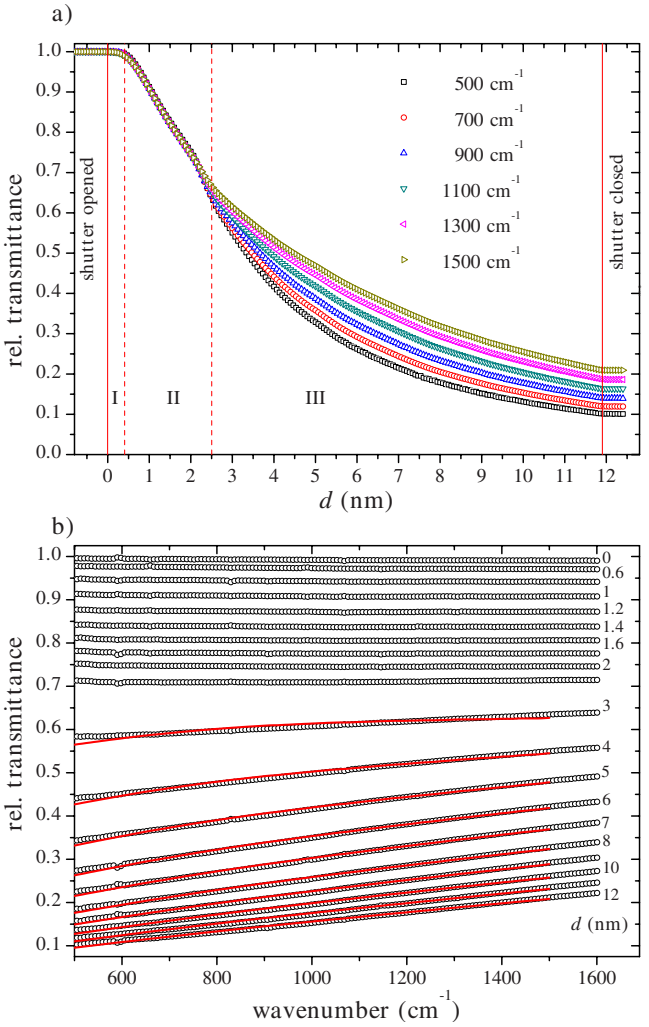

FIG. 1. (Color online) (a) Relative transmittance at different wave numbers versus film thickness for Cr growth on C(100) at room temperature. The three main growth phases are indicated by broken vertical lines. The constant transmittance before opening and after closing the Cr shutter demonstrate the measurement stability. (b) Selection of transmittance spectra recorded during Cr evaporation (open symbols). The continuous lines are best-fit calculations based on the Drude model for $d > 2.5$ nm.

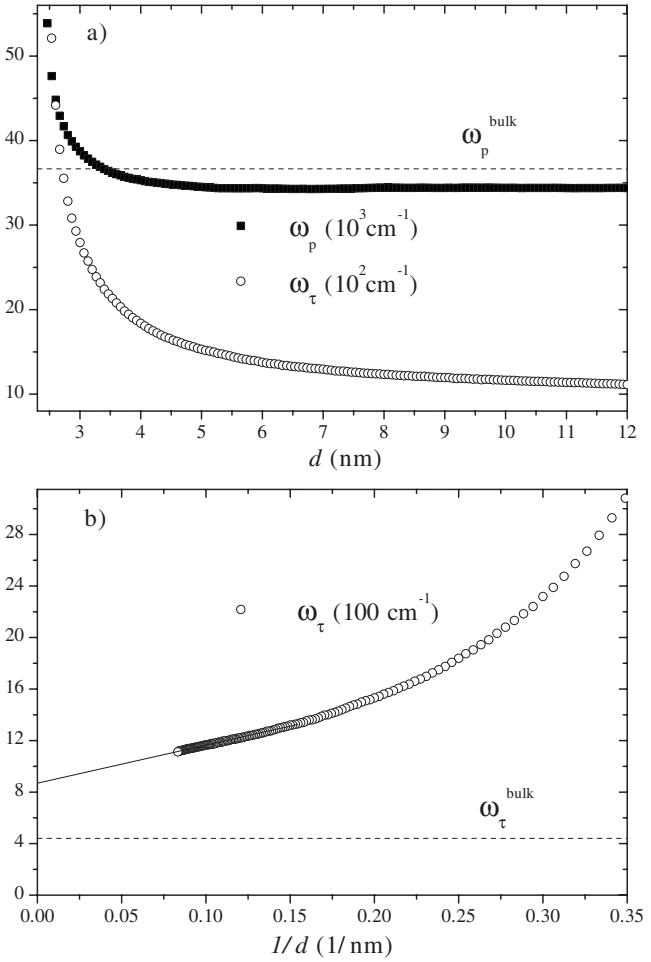

FIG. 2. (a) Drude parameters versus film thickness obtained from best-fit calculations. The diverging parameters for $d \rightarrow 2.5$ nm indicate the breakdown of the free-electron model. (b) ω_τ vs $1/d$. For $d > 6$ nm, ω_τ decreases linearly as expected from CSE. An extrapolation to $d \rightarrow \infty$ yields a value roughly twice $\omega_\tau^{\text{bulk}}$. Bulk values are indicated by broken lines.

thickness for percolation, which in case of metal-island formation gives a percolation threshold that significantly depends on temperature.[7] From percolation on, coalescence and lateral growth of the crystalline area proceed, which results in a clear metallic dispersion in IR transmittance. Comparison of those features of island-like films to the Cr growth observations leads to the only conclusions that Cr film percolation is reached already at the very low-average film thickness of about 0.7 nm and that during further Cr deposition, the nanoislands do not coalesce to bigger grains and do not form a crystalline layer for some reason. Instead, up to the average thickness of ~2.5 nm, the individual islands can grow in their height only. Then, in phase III, for $d > 2.5$ nm, the transmittance increases with increasing wave number, as expected for a Drude-type metal layer.

We will now proceed with a detailed discussion of the dynamic conductivities in phase III and II, and of the transition from II to III. We start with the thickest films since they show well-known Drude-like behavior.

A. Films with Drude-like conductivity

A selection of recorded spectra and respective Drude-fit curves for the range of 500 cm^{-1}–1500 cm^{-1}, based on the dielectric-function from Eq. (1) with ω_p and ω_τ as fit parameters are shown in Fig. 1(b). The fits were performed with the software package *SCOUT*,[34] which exactly considers the thin film optics. Very good accordance for films beyond 2.5 nm is obvious, see Fig. 1(b).

Figure 2(a) displays the obtained Drude parameters. For films with $d < 2.5$ nm, the fit provides unreasonable parameters. The relaxation rate corresponds to a mean free path for the electrons of less than one atomic distance, contradicting the Ioffe-Regel criterion[35] and indicating a breakdown of the free-electron model.

For $d > 2.5$ nm, the Drude-type fit provides reasonable values for the two parameters. ω_p reaches a constant value at

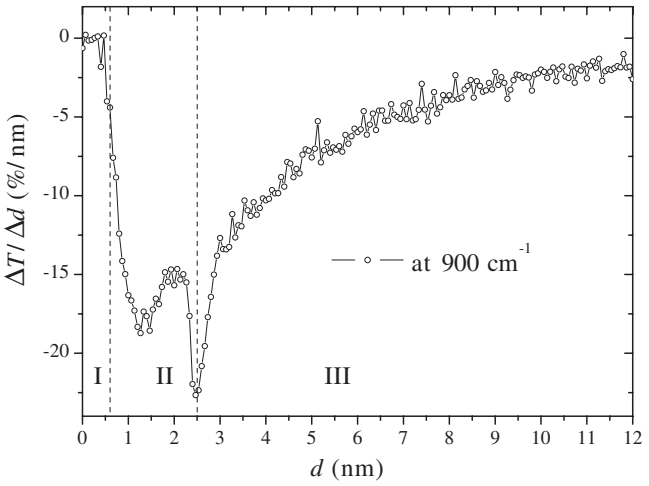

FIG. 3. The derivative of $T(\omega=900\ \mathrm{cm}^{-1})$ with respect to d for Cr growth on diamond. The sharp minimum at $d=2.5$ nm indicates an abrupt, qualitative change in the optical conductivity at this thickness. T was averaged in the interval $880\ \mathrm{cm}^{-1}<\omega<920\ \mathrm{cm}^{-1}$.

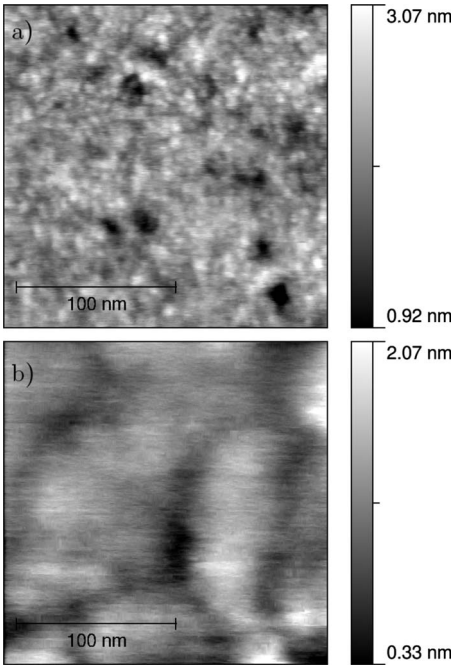

FIG. 4. AFM images ($200\times200\ \mathrm{nm}^2$) of Cr films grown on diamond at room temperature with average thicknesses d of (a) 1.5 nm and (b) 5 nm. Both measurements were performed *ex situ* in contact mode.

higher d. The deviation of only 6% to the bulk value may be related to the error of the thickness calibration. ω_τ becomes linearly dependent on $1/d$ at higher d, as shown in Fig. 2(b). This is expected from the CSE for constant film roughness and structure [see Eq. (3)]. An extrapolation of ω_τ for $1/d$ toward 0 ends up at a more than two times larger value compared to $\omega_\tau^{\mathrm{bulk}}$, indicating a defect rich polycrystalline film with lower dc conductivity than that following from published data of bulk Cr. However, by increasing the substrate temperature to $T=400$ K, the crystalline quality of the Cr films can be significantly improved, which in our IR studies gives spectra that correspond to lower relaxation rates.[36]

B. At the phase transition

At $d=d_{\mathrm{crit}}\approx2.5$ nm both the Drude parameters approach rather high values, see Fig. 2(a). Furthermore, the derivative of the transmittance with respect to the thickness exhibits an extremum at $d=2.5$ nm, as shown in Fig. 3. Both these arguments indicate the strong change in the morphology of the film at d_{crit}. It has to be mentioned that the origin of the sudden spectral change at ~2.5 nm is unlikely a transition from the antiferromagnetic to the paramagnetic state as the Néel-temperature is expected to be well below room temperature for such thin Cr films.[37] Measurements at various different substrate temperatures[36] gave the surprising result that the IR spectra below d_{crit} and d_{crit} itself only negligibly depend on temperature, clearly different to the case of island-like growth where the critical thickness for the transition to a conducting layer is observed to decrease with decreasing temperature and strong spectral changes are observed.[7] The nearly temperature independent d_{crit} also contradicts amorphous growth effects due to hampered diffusion at low temperatures.[38] Accordingly, another reason that is not related to diffusion properties, should exist for the transition from the discontinuous phase to the bcc polycrystalline one. Since good arguments were already given on the energetically favored formation of fcc nanoclusters up to diameters of $d<2.5$ nm, the transition from that phase to the bcc bulk one certainly can be considered as the main reason for the sudden change observed in IR spectra at 2.5 nm. Additional support for this interpretation of a dominant fcc Cr phase in the initial stage of the growth is given by the better lattice match for diamond and fcc Cr. While the mismatch is 14.3% for bcc Cr ($a_{\mathrm{dia}}/\sqrt{2}=2.52$ Å, $a_{\mathrm{bcc\ Cr}}=2.88$ Å), it is only 1.4% for fcc Cr [$a_{\mathrm{dia}}=3.57$ Å, $a_{\mathrm{fcc\ Cr}}=3.62$ Å (Ref. 39)]. Our AFM data presented in Fig. 4 corroborate our interpretation of the phase transition. While for $d<d_{\mathrm{crit}}$ the AFM image shows small, uniform nanoparticles, for $d>d_{\mathrm{cit}}$ expanded homogeneous structures are observed. Unfortunately, the precise value for the nanoparticle size cannot be directly taken from the image, since it represents a convolution of the tip contour and the nanoparticle geometry. However, the obvious nanoparticle size in the image can be considered as the upper limit of the real size and, thus, is in agreement to the prediction for critical cluster size.

C. Conductivity of the discontinuous phase

According to the above mentioned arguments phase II certainly consist of densely packed nanocrystals and is therefore not amorphous. Accordingly, the conductivity should not be fully suppressed due to charge carrier localization. Indeed, the extremely weak frequency dependence of IR transmittance in phase II rather points to a nonvanishing static conductivity[40] than to an insulating behavior. Because of these two reasons we tried to get useful conductivity parameters from spectral fits to the Drude-Smith model which, in contrast to the Drude model, accounts for coherent back-

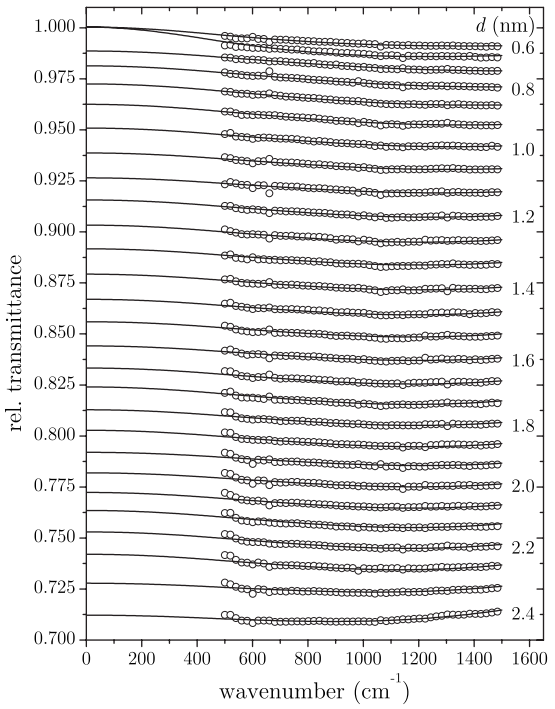

FIG. 5. Comparison between measured spectra (open symbols) and Drude-Smith model (continuous lines, extrapolated to static case) for $d<2.5$ nm. The film thickness is indicated on the right for every third spectrum.

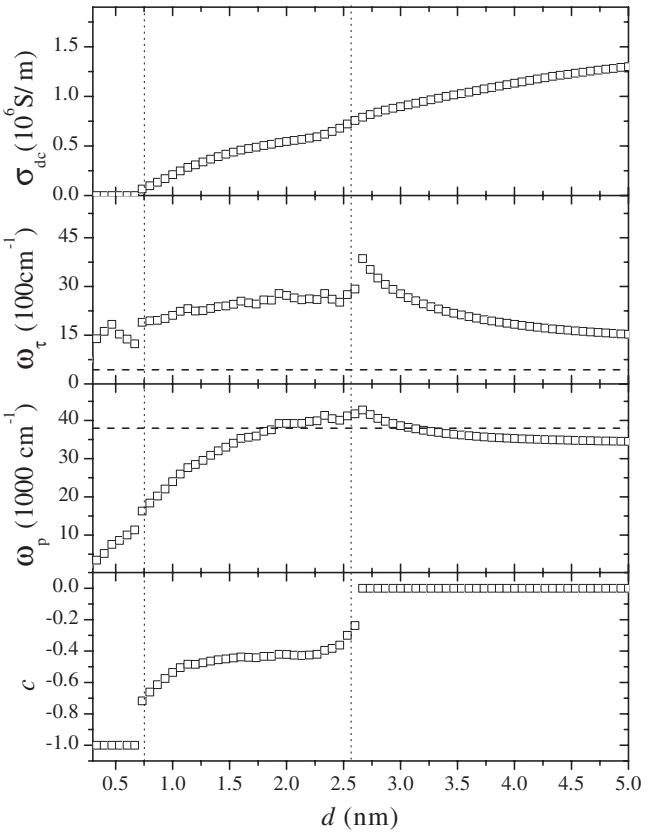

FIG. 6. Parameters obtained from best fit with Drude-Smith model for the dielectric function versus Cr thickness in phase II and III and respective dc conductivity. Bulk values for bcc Cr are shown as broken lines.

scattering effects as they may occur in a dense package of nanocrystallites.

Fit results from the Drude-Smith model for spectra of films with $d<d_{\mathrm{crit}}$ are shown in Fig. 5. Excellent accordance between calculations (based on Eq. (4)) and experimental data is obvious. It has to be noticed that fits with Drude-Smith model beyond the single-scattering approximation do not improve the accordance to experiment. Figure 5 also shows the extrapolation of the fit curves to the dc limit. The dc values with relative transmittance <1 (and thus, with $\sigma_{\mathrm{dc}}>0$) indicate conductive layers from 0.7 nm on.

Figure 6 summarizes the Drude-Smith parameters for the whole thickness range. The persistence of velocity parameter c equals -1 for the transition from phase I to phase II before steeply rising to ~ -0.5 in phase II. There, from about 1 nm on, the parameter stays nearly unchanged for a range of 1.5 nm before rising abruptly to a value close to zero. Au on Si produced by cluster deposition was reported to show similar behavior in c.[30] The results can be interpreted in the following way: when $c=-1$ the dc conductivity of a film is completely suppressed, while for $-1<c<0$ the dc conductivity is nonzero.[26] The specially interesting finding is the constant value for c of around -0.5 over a rather broad thickness range. It indicates backscattering of the same amount while the average film thickness is increasing. An explanation could be this: Densely packed fcc Cr nanoislands grow in height under conservation of the lateral structure and, therefore, the measured in-plane conductivity is marginally effected. As it could be seen from the values given in Fig. 6, the parameters ω_{p} and ω_{τ} of the Drude-Smith-type fit correspond to reasonable values throughout the whole film growth. In phase II, the increasing value of ω_{p} is not related to the Drude-Smith model. Instead it could be a hint that quantum size effects strongly alter the carrier density, as it is expected for films in that thickness range, where d is comparable to the wavelength of the electrons.[22] The overshoot of ω_{p} above $\omega_{\mathrm{p}}^{\mathrm{bulk}}$ for $2\ \mathrm{nm}<d<2.5$ nm corresponds to a higher plasma frequency for fcc Cr compared to bcc Cr, an assumption supported by calculations in Ref. 41. For $d<d_{\mathrm{crit}}$, ω_{τ} changes only slightly. At d_{crit}, ω_{τ} exhibits a discontinuity as expected at an electronic percolation transition.[29] Since c is very close to 0 for $d>2.5$ nm, the results from the Drude-like fit are reproduced for ω_{p} and ω_{τ} in this thickness range. So, for phase II, the successful Drude-Smith-type fits to a series of spectra demonstrate that it is possible to describe experimental IR spectra of an unusual phase with reasonable parameters.

V. SUMMARY

In summary, with sensitive IR spectroscopy during film growth a structural phase transition in ultrathin chromium was observed at a film thickness of 2.5 nm. At higher thickness, the Cr films show the Drude-type behavior with a relaxation rate that is modified according to the classical size

effect. The critical thickness itself and the IR spectral properties of the Cr films at lower thickness corroborate the old theoretical finding of preferred fcc nanocluster formation. The sequence of IR spectra of that phase can be well described with the Drude-Smith model. The respective fit parameters represent reasonable values, as explained, and, moreover, the special parameter c indicates partially coherent backscattering of electrons, which may be seen as indicative of the nanocrystalline array.

ACKNOWLEDGMENTS

R.L. acknowledges an inspiring discussion with M. Walther and financial support by the EU under Project No. RII3-CT-2004-506078, Integrated Infrastructure Initiative Hadron Physics, and the Gesellschaft für Schwerionenforschung (GSI), Darmstadt. Both authors thank E. Berdermann (GSI) for a fruitful collaboration.

*Author to whom correspondence should be addressed; pucci@kip.uni-heidelberg.de

[1] S. M. Durbin, L. E. Berman, B. W. Batterman, M. B. Brodsky, and H. C. Hamaker, Phys. Rev. B **37**, 6672 (1988).
[2] L. Saraf, C. Wang, M. H. Engelhard, and D. R. Baer, Appl. Phys. Lett. **82**, 2230 (2003).
[3] M. B. Brodsky, P. Marikar, R. J. Friddle, L. Singer, and C. H. Sowers, Solid State Commun. **42**, 675 (1982).
[4] D. Tomanek, S. Mukherjee, and K. H. Bennemann, Phys. Rev. B **28**, 665 (1983).
[5] S. H. Huh, H. K. Kim, J. W. Park, and G. H. Lee, Phys. Rev. B **62**, 2937 (2000).
[6] E. Berdermann, M. Ciobanu, S. H. Connell, A. M. O. D. da Costa, L. Fernandez-Hernando, A. Oh, and J. P. F. Sellschop, Phys. Status Solidi A **201**, 2521 (2004).
[7] F. Meng and A. Pucci, Phys. Status Solidi B **244**, 3739 (2007).
[8] G. Fahsold and A. Pucci, *Advances in Solid State Physics* (Springer-Verlag, Berlin/Heidelberg, 2003), Vol. 43, pp. 833–847.
[9] G. Fahsold, A. Priebe, A. Pucci, and A. Otto, *Epioptics 8: Proceedings of the 33rd Course of the International School of Solid State Physics* (World Scientific, Singapore, 2004), pp. 159–166.
[10] G. Fahsold, M. Sinther, A. Priebe, S. Diez, and A. Pucci, Phys. Rev. B **65**, 235408 (2002).
[11] G. Fahsold, M. Sinther, A. Priebe, S. Diez, and A. Pucci, Phys. Rev. B **70**, 115406 (2004).
[12] A. Pucci, F. Kost, G. Fahsold, and M. Jalochowski, Phys. Rev. B **74**, 125428 (2006).
[13] S. Berthier, J. Peiro, S. Fagnent, and P. Gadenne, Physica A **241**, 1 (1997).
[14] M. Jałochowski and E. Bauer, Phys. Rev. B **38**, 5272 (1988).
[15] K. Budde, E. Abram, V. Yeh, and M. C. Tringides, Phys. Rev. B **61**, R10602 (2000).
[16] Z. Kuntová, M. C. Tringides, and Z. Chvoj, Phys. Rev. B **78**, 155431 (2008).
[17] C. A. Jeffrey, E. H. Conrad, R. Feng, M. Hupalo, C. Kim, P. J. Ryan, P. F. Miceli, and M. C. Tringides, Phys. Rev. Lett. **96**, 106105 (2006).
[18] S. S. Fouad, A. H. Ammar, and M. H. El-Fazary, Phys. Status Solidi B **187**, 99 (1995).
[19] G. Fahsold, A. Bartel, O. Krauth, N. Magg, and A. Pucci, Phys. Rev. B **61**, 14108 (2000).
[20] E. H. Sondheimer, Adv. Phys. **1**, 1 (1952).
[21] A. Matthiessen and M. von Bose, Ann. Phys. Chem. **191**, 353 (1862).
[22] N. Trivedi and N. W. Ashcroft, Phys. Rev. B **38**, 12298 (1988).
[23] D. V. Fedorov, G. Fahsold, A. Pucci, P. Zahn, and I. Mertig, Phys. Rev. B **75**, 245427 (2007).
[24] A. Bittar, S. Berthier, and J. Lafait, J. Phys. (Paris) **45**, 623 (1984).
[25] N. W. Ashcroft and N. D. Mermin, *Solid State Physics* (Thomson Learning, Singapore, 2006).
[26] N. V. Smith, Phys. Rev. B **64**, 155106 (2001).
[27] T. Brandt, M. Hövel, B. Gompf, and M. Dressel, Phys. Rev. B **78**, 205409 (2008).
[28] D. G. Cooke, A. N. MacDonald, A. Hryciw, J. Wang, Q. Li, A. Meldrum, and F. A. Hegmann, Phys. Rev. B **73**, 193311 (2006).
[29] M. Walther, D. G. Cooke, C. Sherstan, M. Hajar, M. R. Freeman, and F. A. Hegmann, Phys. Rev. B **76**, 125408 (2007).
[30] A. Thoman, A. Kern, H. Helm, and M. Walther, Phys. Rev. B **77**, 195405 (2008).
[31] M. Yokoba, Y. Koide, A. Otsuki, F. Ako, T. Oku, and M. Murakami, J. Appl. Phys. **81**, 6815 (1997).
[32] A. Priebe, M. Sinther, G. Fahsold, and A. Pucci, J. Chem. Phys. **119**, 4887 (2003).
[33] A. Liebsch and B. N. J. Persson, J. Phys. C **16**, 5375 (1983).
[34] W. Theiss Hard- and Software, *SCOUT*, Aachen, Germany.
[35] A. F. Ioffe and A. R. Regel, *Progress in Semiconductors* (Heywood & Company, London, 1960), Vol. 4, pp. 237–291.
[36] R. Lovrinčić, Doctoral thesis, Ruprecht-Karls-Universität, 2009.
[37] H. Zabel, J. Phys.: Condens. Matter **11**, 9303 (1999).
[38] P. F. Henning, C. C. Homes, S. Maslov, G. L. Carr, D. N. Basov, B. Nikolić, and M. Strongin, Phys. Rev. Lett. **83**, 4880 (1999).
[39] G. Y. Guo and H. H. Wang, Phys. Rev. B **62**, 5136 (2000).
[40] F. J. Wegner, Z. Phys. B **25**, 327 (1976).
[41] J.-h. Xu, A. J. Freeman, T. Jarlborg, and M. B. Brodsky, Phys. Rev. B **29**, 1250 (1984).